Far-red luminescent ruthenium pyridylimine complexes; building blocks for multinuclear arrays†

Anna C. G. Hotze,[a,b] Jonathan A. Faiz,[a] Nikolaos Mourtzis,[b,c] Gabriel I. Pascu,[a,b] Philip R. A. Webber,[b] Guy J. Clarkson,[b] Konstantina Yannakopoulou,[c] Zoe Pikramenou*[a] and Michael J. Hannon*[a,b]

Received 20th December 2005, Accepted 6th April 2006
First published as an Advance Article on the web 13th April 2006
DOI: 10.1039/b518027a

Ruthenium(II) pyridylimine complexes are explored for their potential as units that might be incorporated into electronic or photonic arrays. The complexes $[Ru(bipy)_2(L)][PF_6]_2$ (**1**) and $[Ru(tpy)(L)Cl][BF_4]$ (**2**) with L = phenylpyridin-2-ylmethylene-amine are synthesized and fully characterised using X-ray diffraction analysis and (2D) NMR spectroscopy. **1** displays emission in the far-red area of the spectrum at room temperature. The emission is significantly shifted to longer wavelength with respect to $[Ru(bpy)_3]^{2+}$ indicating that the lowest MLCT state is localised on the pyridylimine ligand. **2** is non-emissive at room temperature and at 77 K.

Introduction

Pyridylimine units[1] are attractive ligands as they have similar properties to the much explored bipyridine[2] ligands (N_2 diimine donor sets and available π-bonding orbitals) yet are much simpler to prepare. We have recently been exploring the potential of pyridylimine ligands for metallo-supramolecular assembly of complex architectures.[3] The ease-of-preparation of these ligands allows ready access to a wide variety of architectures and we have shown that the ligand design can be used to encode subtle features which determine the precise micro-architecture of the arrays. Moreover we have demonstrated that this control of supramolecular architecture can be used to encode functions such as recognition of the DNA major groove.[4]

While architecture assembly is a fascinating application of polypyridine ligands, their enduring popularity arises primarily from their ruthenium complexes, such as the prototypical $[Ru(bpy)_3]^{2+}$ cation, which exhibit exciting photochemical and photophysical properties.[5] Indeed the field of inorganic supramolecular photochemistry[6] remains dominated by multinuclear ruthenium polypyridyl complexes linked either covalently[7] or non-covalently.[8,9] Such complexes are being employed in light-harvesting devices[10] and designed into nano-scale electronic and photonic arrays.[11] The complexes have also been developed as DNA binding agents, particularly when an intercalating agent is incorporated into the molecular design.[12]

The advantages that our readily prepared pyridylimine ligand systems have brought to design of functional supramolecular architectures,[3] might also be of benefit in design of multinuclear photoactive ruthenium complexes for nano-electronics and photonics and we have embarked on a programme to explore such application. We were surprised to discover that, despite the many mononuclear ruthenium polypyridyl complexes that have been investigated, there are few reports[13–17] of ruthenium pyridylimine complexes and so to initiate our investigations we chose first to explore the properties of simple mononuclear complexes to confirm their potential photoactivity. This is particularly pertinent since the addition of aryl rings adjacent to the nitrogens in bipyridines and phenanthrolines leads to a dramatic loss of photoactivity.[18,19] We report herein the synthesis and characterisation (in both solid state and solution) of mononuclear ruthenium(II) pyridylimine complexes containing bipyridine and terpyridine co-ligands, and demonstrate that the ruthenium bipyridine complex displays emission in the far-red area of the spectrum at room temperature, whilst the terpyridine complex displays no emission at room temperature or 77 K.

Several examples of mononuclear ruthenium complexes containing terpyridine and phenylazopyridine ligands[20–23] or 2,2′-azobispyridine[24] are known in literature. Only a few reports are known of ruthenium complexes with both terpyridine and pyridylimine-based ligands.[15,16] Previous reports of ruthenium(II) tris-diimine complexes containing bipyridine and pyridylimine ligands are few and occasionally appear contradictory. Meyer *et al.*[25] reported what was probably the first example by electrochemical oxidation of the corresponding pyridylmethylamine complex to yield $[Ru(bpy)_2(C_5H_5NCHNH)]^{2+}$. Belser and von Zelewsky[26] and Maruyama and Kaizu[13] described a similar complex with the alkyl pyridylimine ligand prepared from methylamine. Dose and Wilson[27] studied the pyridylimine ligand derived from 4-tolylamine but reported that mixed ligand complexes could not be prepared by direct reaction with $[Ru(bpy)_2Cl_2]$. However, Choudhury *et al.*,[17] using a silver(I) mediated synthesis, subsequently obtained this mixed complex in low yield, after chromatographic purification to remove side-products. They report the complex to be non-emissive at room temperature. More recently Yam and Lee[28] have prepared a mixed ligand complex from the pyridylimine

[a]*School of Chemistry, The University of Birmingham, Edgbaston, Birmingham, UK B15 2TT. E-mail: m.j.hannon@bham.ac.uk, z.pikramenou@bham.ac.uk; Fax: +44 121 414 7871; Tel: +44 121 414 2527/2290*
[b]*Centre for Supramolecular and Macromolecular Chemistry, Department of Chemistry, University of Warwick, Gibbet Hill Road, Coventry, UK CV4 7AL*
[c]*Institute of Physical Chemistry, National Centre for Scientific Research "Demokritos", 15310, Aghia Paraskevi, Greece*

† Electronic supplementary information (ESI) available: Fig. S1 and S2. See DOI: 10.1039/b518027a

ligand of an arylamino azacrown and Meade *et al.*[29] have prepared complexes of alkyl linked pyridylimine-nucleotides. Both report room temperature emission. Brunner *et al.*[30] have described the formation of diastereomeric mixed ligand complexes from a chiral pyridylimine ligand and chromatographically separated the two diastereoisomers, one of which was crystallographically characterised.

Results and discussion

Synthetic considerations of ligand L

The ligand L (Fig. 1) was selected since it contains an aryl residue linked directly into the pyridylimine binding unit. Although the previous literature appeared to indicated that ruthenium complexes of alkyl substituted pyridylimines were both more accessible and more likely to be photoactive, we specifically investigated this aryl substituted pyridylimine as in our ultimate multinuclear designs we plan to incorporate conjugated links for effective electronic and photonic communication. Moreover conjugation of an aryl with the pyridylimine unit can dramatically enhance the stability of the imine bond and this can affect the chemistry. The ligand was prepared by stirring pyridine-2-carbaldehyde and phenylamine in benzene at room temperature in the presence of 3 Å molecular sieves (to remove water, one of the condensation products). The molecular sieves were removed by filtration and the solvent removed *in vacuo* to yield the crude ligand as an oil which was reacted on without further purification.

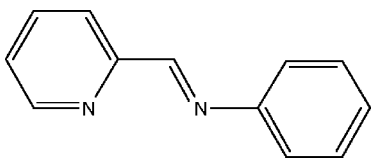

Fig. 1 The structure of pyridylimine ligand L.

The FAB mass spectrum of ligand L shows a single peak corresponding to $\{LH\}^+$ and the IR spectrum shows peaks corresponding to imine and aromatic stretches. The ^{1}H NMR spectrum was recorded in acetone-d_6 and shows a singlet at 8.58 ppm corresponding to the imino proton and confirming the formation of the desired imine bond. The rest of the peaks follow the typical patterns of a pyridyl and a monosubstituted phenylene moiety, and are readily assigned from their splitting patterns, the coupling constants and the integration. The assignment was confirmed by 2D COSY NMR spectroscopy. There are some minor peaks in the spectra corresponding to about ~5% of starting amine and aldehyde; imine bonds are susceptible to hydrolysis in the free ligands and this observation is unsurprising.

Synthesis, characterisation and luminescent properties of $[Ru(bipy)_2(L)][PF_6]_2$ (1). The complex $[Ru(bipy)_2(L)][PF_6]_2$ (**1**) was prepared by reacting L with *cis*-$[Ru(bipy)_2Cl_2]$ in methanol solution under reflux, to afford a red-brown solution. After cooling to room temperature, the solution was treated with excess methanolic ammonium hexafluorophosphate to yield a red-brown precipitate of **1**. Despite the reports of Dose and Wilson[27] and Choudhury *et al.*[17] with the tolyl analogue, with this ligand the reaction proceeded cleanly in good yield with need neither for silver(I) to remove the chloride nor chromatography to purify the product. The IR spectrum of **1** shows peaks corresponding to the imine and aromatic stretches and the hexafluorophosphate counterion. The FAB-MS data for (**1**) shows peaks at m/z = 741 and 596, corresponding to $\{[Ru(bipy)_2L](PF_6)\}^+$ and $\{[Ru(bipy)_2L]\}^+$ respectively, consistent with the expected formulation $[Ru(bipy)_2L](PF_6)_2$; partial elemental analysis is also consistent with this proposed formulation. Recrystallisation of the complex by slow diffusion of diisopropylether into an acetonitrile solution of the salt afforded crystals suitable for X-ray crystallography.

The crystal structure (Fig. 2) reveals the expected six-coordinate ruthenium(II) centre surrounded by five pyridine nitrogens and one imino nitrogen. The bond lengths to the bipyridine nitrogens (Ru–N 2.057–2.077 Å) are unremarkable and similar to those observed in the $[Ru(bipy)_3]^{2+}$ cation (2.056 Å).[31] The bond to the pyridine of the pyridylimine ligand is also similar (2.056 Å) while that to the imine nitrogen is slightly shorter (2.045 Å). The bipyridine units are essentially planar (torsion angles between the rings 7.5 and 4.5°) as is the pyridylimine unit (torsion angle 1.5°). The phenyl ring is twisted through 45° with respect to the pyridylimine unit. This phenyl unit is positioned above a pyridyl ring of an adjacent bipyridine, however the geometric constraints at the imine nitrogen mean that it is not stacked coplanar with (or perpendicular to) that pyridyl ring. The tris chelate cation is chiral and both enantiomers are observed in the solid-state structure. In the structure there are columns of cations with the same helicity, and adjacent columns alternate in helicity. The hexafluorophosphate anions are packed between these columns and form a number of short contacts to the protons on the ligands. There are no face–face π–π interactions within or between the cations and, somewhat surprisingly, nor are there extensive face–edge (CH···π) interactions between the cations.

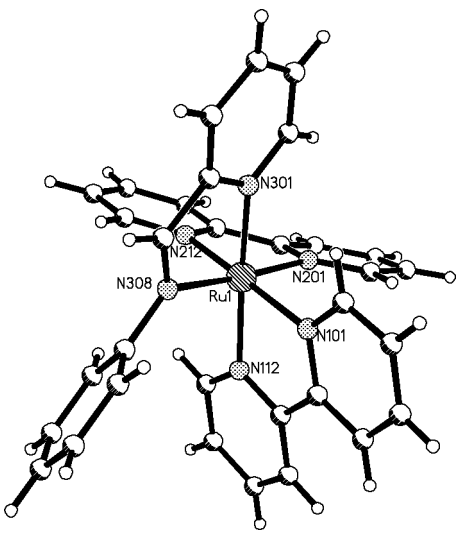

Fig. 2 Structure of the cation **1**.

It is instructive to compare the coordination environment observed in this pyridylimine complex with that observed in the crystallographically characterised $[Ru(bipy)_2(tpy\text{-}N,N')]^{2+}$ cation (in which the terpyridine ligand acts as a bidentate ligand with a non-coordinated pyridyl ring); the structure of $[Ru(bipy)_2(Phbpy)]^{2+}$ is

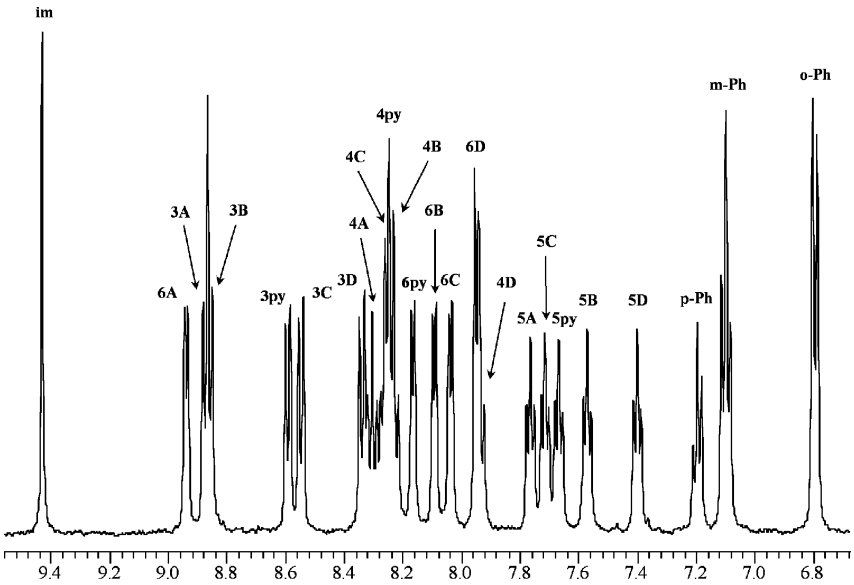

Fig. 3 500 MHz ^{1}H NMR spectrum of $[Ru(bipy)_2(L)][PF_6]_2$ in acetone-d_6 solution at 298 K.

expected to be analogous.[19] In that structure the non-coordinated ring was stacked coplanar above another pyridine ring, however the steric constraints needed to accommodate the non-coordinated ring resulted in elongation of the Ru–N bonds to the tpy. This is not the case in this pyridylimine containing cation whose coordination environment is more like that of $[Ru(bipy)_3]^{2+}$.

The ^{1}H NMR spectrum of the diamagnetic complex **1** was recorded in acetone-d_6 solutions at 298 K and is illustrated in Fig. 3. Connectivity within the pyridyl and phenyl rings was established using 2D COSY NMR experiments. There are five different pyridine moieties; one derived from ligand L and four from the two non-equivalent bipy ligands. The chemical shifts of the pyridyl protons are collected in Table 1 together with those of $[Ru(bipy)_3]^{2+}$ (also a numbering scheme is given). 2D NOESY NMR experiments enabled the connectivity between the imine, pyridyl and phenyl units to be established with cross peaks observed between H_{im}–H_{3py}; H_{im}–$H_{oPh;}$ H_{3C}–H_{3D}. H_{3A} and H_{3B} are too close in chemical shift to observe an NOE between them with any certainty, but they do not show NOEs to the other H_3 protons or the imino or phenyl protons. The comparison of the chemical shifts of the bpy rings with those observed for the $[Ru(bipy)_3]^{2+}$ cation is revealing. The chemical shifts of the protons in rings A and B are very similar to those of $[Ru(bipy)_3]^{2+}$ except for H_{6A} which is shifted dramatically downfield by 0.8 ppm. NOESY cross peaks are observed between this proton and weakly to the imino proton (H_{im}) and strongly to the ortho proton of the phenyl ring confirming that this proton is the one located above the imine unit and this establishes the absolute assignment of rings A and B. The dramatic downfield shift is accounted for by the absence of the pyridyl ring current shift experienced by H_6 of the other rings. For ring C, the shifts of protons 6 and 4 are unremarkable while proton 3 and all the protons of ring D are shifted upfield with respect to the corresponding protons in $[Ru(bipy)_3]^{2+}$. These are the protons over which the phenyl ring is located and they experience the ring current of this residue. This assignment is confirmed by NOESY cross peaks from H_{6D} to the *ortho* proton of the phenyl ring, which establish the absolute assignment of rings D and C. The protons of the phenyl ring are sharp indicating that the phenyl ring is rotating freely in solution at room temperature. This is in contast to the non-coordinated rings in the $[Ru(bpy)_2(tpy\text{-}N,N')]^{2+}$ and $[Ru(bpy)_2(Phbpy)]^{2+}$ cations[19] which experience restricted rotation and again emphasises the difference between the complexes of this aryl substituted pyridylimine and those of analogous aryl substituted bipyridines. This assigment using 2D NOESY NMR is in agreement with the assignment for the structural related $[Ru(bpy)_2(azpy)](PF_6)_2$ compound (azpy = 2-phenylazopyridine).[32]

Table 1 ^{1}H NMR chemical shift (δ) data for the pyridyl protons in $[Ru(bipy)_2(L)]^{2+}$ and $[Ru(bipy)_3]^{2+}$ in acetone-d_6 solution at 298 K

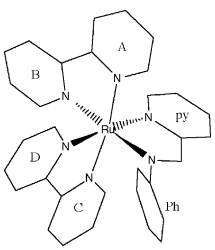

		H_6	H_5	H_4	H_3
$[Ru(bipy)_2(L)]^{2+}$	py of pyim	8.17	7.67	8.25	8.59
	bpy A	8.94	7.76	8.31	8.87
	bpy B	8.09	7.57	8.25	8.86
	bpy C	8.04	7.71	8.25	8.55
	bpy D	7.94	7.40	7.94	8.34
$[Ru(bipy)_3]^{2+}$		8.07	7.59	8.23	8.83

The electrochemical behaviour of the complex in acetonitrile solution has been examined by cyclic voltammetry. Solutions of $[Ru(bpy)_2(L)]^{2+}$ show a reversible ruthenium(II)/(III) oxidation at +0.96 (*vs.* Fc/Fc^+). This is slightly higher than the value of +0.85 V reported[5,19] for the $[Ru(bpy)_3]^{2+}$ and $[Ru(bpy)_2(Phbpy)]^{2+}$ cations and +0.91 V for the $[Ru(bpy)_2(tpy\text{-}N,N')]^{2+}$ cation and implies that the pyridylimine ligand slightly stabilises the ruthenium(II) oxidation state (compared to bipyridine) which may reflect enhanced

π-back donation to this ligand, which would be consistent with the slightly shorter Ru–N bond to the imino nitrogen observed in the X-ray crystal structure. Four reversible reductions are observed at −1.41 V and −1.92 V and −2.11 V and −2.23 V (*vs.* Fc/Fc^+). The reductions in such systems are known to be ligand centred rather than ruthenium centred and comparing these reduction potentials with those of $[Ru(bpy)_2(tpy\text{-}N,N')]^{2+}$ (−1.69 V and −1.91 V) and $[Ru(bpy)_2(Phbpy)]^{2+}$ (−1.76 V and −1.91 V)[19] it is apparent that the pyridylimine ligand is more easily reduced than the bipyridines and that the first ligand centred reduction takes place at L.

The absorption spectrum of an acetonitrile solution of $[Ru(bpy)_2(L)]^{2+}$ shows a very broad absorption band between 400–530 nm with a structure that indicates two overlapping bands with maxima around 440 nm ($\varepsilon \sim 9\,000$ dm^3 mol^{-1} cm^{-1}) and 480 nm ($\varepsilon \sim 9\,000$ dm^3 mol^{-1} cm^{-1}) (Fig. 4). This may be compared with[5,19] the absorption maxima at $\lambda = 452$ nm ($\varepsilon = 13\,000$ dm^3 mol^{-1} cm^{-1}) for $[Ru(bpy)_3]^{2+}$ at $\lambda = 450$ nm ($\varepsilon = 12\,000$ dm^3 mol^{-1} cm^{-1}) for $[Ru(bpy)_2(tpy\text{-}N,N')]^{2+}$ and at 447 nm ($\varepsilon = 10\,000$ dm^3 mol^{-1} cm^{-1}) for $[Ru(bpy)_2(Phbpy)]^{2+}$. A red shift of the ^{1}MLCT absorption band in Ru(II) complexes on replacing pyridine ligands with imines has been previously noted[13,17,33] and is consistent with the electrochemical results that suggest that the pyridylimine ligand has a lower energy π* level than the bipyridine ligand. In addition to the broad 400–530 nm band a shoulder at ~350 nm ($\varepsilon \sim 7\,000$ dm^3 mol^{-1} cm^{-1}) is evident on the edges of the 280 nm ligand-based band.

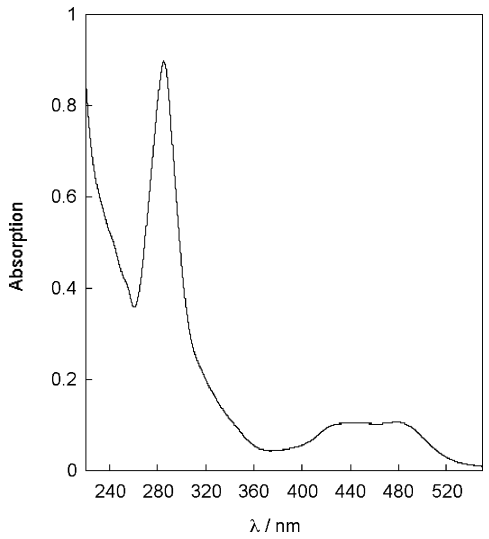

Fig. 4 Absorption spectrum of **1** in CH_3CN (2.3×10^{-5} M).

Upon excitation at 440 or 480 nm complex **1** exhibits a broad weak emission centred at 770 nm which is assigned to a ^{3}MLCT transition (Fig. 5). The excitation spectrum (monitored at 770 nm) displays a profile of the two overlapping bands in the visible 440 and 480 nm and a broad UV profile. This confirms that the emission originates from population of the ^{1}MLCT states. Excitation of the complex in a rigid glass at 77 K leads to a sharper and blue shifted emission profile with an emission maximum at 730 nm (Fig. 5). The unusual appearance of a luminescence signal from a Ru(II) complex at the far-red region of the visible is consistent with the electrochemical and optical properties of the complex, indicating that the lowest MLCT state is localised

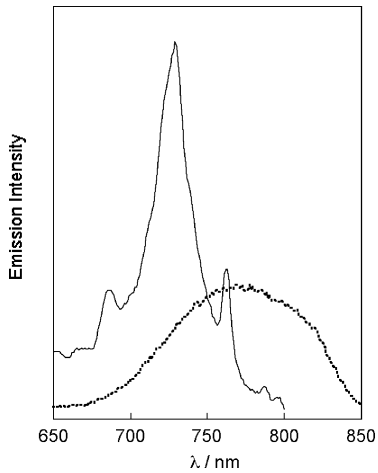

Fig. 5 Luminescence spectra of **1** in CH_3CN at RT (dotted line), and in BuCN–MeCN (4 : 1) (solid line) $\lambda_{exc} = 440$ nm, recorded with a 750 nm grating on the emission monochromator. The RT spectrum is not corrected for PMT response. Intensities are not normalised.

on the imine ligand L.[13,33] The 140 nm red shift compared to $[Ru(bpy)_3]^{2+}$ might be attributed to C=N bond distortion in the excited state.[13] The samples used for the emission studies were recrystallised and were single-crystal samples. The luminescence lifetimes of the 770 nm band in aerated or degassed solutions are shorter than the instrument response (50 ns). The short lifetime of the 770 nm band, attributed to the ^{3}MLCT, is not surprising due to the low energy of that state that leads to fast decay to the ground state. However, acetonitrile solutions of **1** displayed an additional emission band at 520 nm following excitation at 360 nm (see Electronic Supplementary Information, ESI†). The emission intensity at 520 nm increased on addition of HCl or to a lesser extent on addition of Et_4NCl, while the emission at 770 nm was unaffected by this and no detectable change in the UV-Vis absorption spectra was observed.[34] The excitation spectrum monitored at 520 nm reveals a band at 360 nm to be responsible for leading to this emission (see ESI†). In previous studies of Ru(II) complexes with imine ligands, there is one brief mention of multiple band emission spectra[17] at low temperature, however only preliminary studies were reported and their two emission wavelengths were quite similar to each other. A possibility may be that this green emission is attributed to an intraligand charge transfer state, although in the UV-Vis spectrum we cannot unequivocally assign this band. To further investigate the origin of this green emission, and its unusual sensitivity to environment we performed a series of control experiments. We can exclude the 520 nm emission arising from traces of $[Ru(bpy)_3]^{2+}$ ($\lambda_{em} = 630$ nm) or the free ligand (which emits at 330 nm) but we cannot exclude the formation of a species upon irradiation that may lead to an emission at this range of the spectrum. Photosubstitution is known for Ru polypyridylimine complexes although this is most usually associated with complete loss of a bidentate ligand.[35] If that were the case in our systems, $[Ru(bpy)_2(MeCN)_2]^{2+}$ would be formed. The complex $[Ru(bpy)_2(MeCN)_2]^{2+}$ is reported to emit at 77 K at 542 nm.[5] The increased flexibility of the pyridylimine ligand (compared to bpy) might allow a monosubstitution instead, that would give rise to green emission upon prolonged irradiation

and formation of species arising from partial substitution of the pyridylimine ligand (didentate to monodentate) with one acetonitrile ligand.[36]

Synthesis and characterisation of [Ru(tpy)(L)Cl][BF_4] (2). [Ru(tpy)(L)Cl][BF_4] (**2**) was prepared by reaction of [Ru(tpy)Cl_3][37] with one equivalent of L in refluxing methanol, in the presence of 4-ethylmorpholine. Subsequent treatment with ammonium tetrafluoroborate afforded the dark purple complex **2**. The IR spectrum of **2** shows peaks corresponding to the imine and aromatic stretches and the tetrafluoroborate counterion. The FAB mass spectrum of (**2**) shows a strong peak at m/z = 552, corresponding to [Ru(tpy)LCl]$^+$. While [Ru(tpy)(bpy)Cl]$^+$ exists as a single isomer, the asymmetry of the ligand L means that two possible geometric isomers are possible depending on the orientation of L with respect to the chloride ligand (shown schematically in Fig. 6). The position adjacent to the chloride might either be occupied by the pyridine (A) or the imine (B). Steric interactions between the phenyl ring and the chloride might favour isomer (A).

The ^{1}H NMR spectrum of **2** (Fig. 7) reveals that although both isomers are present (as shown by examining the reaction mixture by NMR before adding the counterion) one of the two isomers predominates on precipitating the compound as BF_4 salt. To investigate this further the reaction was repeated and the reaction mixture taken to dryness, rather than being treated with tetrafluoroborate anions. An ^{1}H NMR spectrum of the solid residue indicated the isomer ratio (A : B) to be approximately 4 : 1.

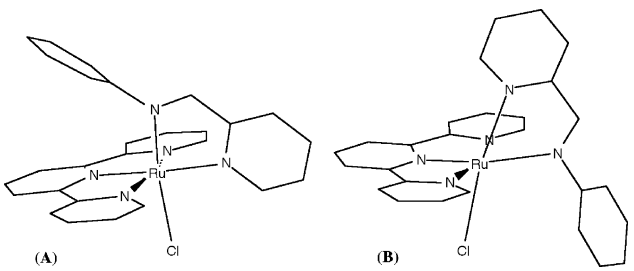

Fig. 6 Schematic representation of the two possible isomers for complex cation **2**.

The identity of the major isomer is readily assigned from the ^{1}H NMR spectrum. The observation of doublet at high frequency (10.26 ppm) immediately confirms this isomer to be isomer (A). The doublet corresponds to H_6 of L and is typical for a pyridine H_6 located *cis* to, and oriented towards, a coordinated chloride.[38] Only in isomer (A) is there a pyridine H_6 proton in such a position and orientation (*vide infra*). The spectrum is readily assigned from the coupling constants and relative integrals. 2D COSY experiments confirm the connectivity within the rings and the expected NOEs are observed in 2D NOESY experiments between H_3 and $H_{3'}$ in the tpy ligand and between H_{im} and both H_o and H_3 in ligand L, confirming the connectivity between the rings. A further NOE is observed between H_o on the phenyl ring and H_6 of the tpy confirming that the phenyl ring is located on top of the tpy ligand and that the isomer is (A). A further NOE between H_6 of L and H_6 of the tpy is also consistent with isomer (A). Moreover, the chemical shifts of the central tpy ring are similar to those of the corresponding ring in [Ru(tpy)(bpy)Cl]$^+$ and in stark contrast to those in [Ru(tpy)(Phbpy)Cl]$^+$ which experience a dramatic upfield shift as a consequence of a stacked phenyl ring.[38] Thus in solution the phenyl ring (which is rotating freely at room temperature) lies above the tpy ligand but is not π-stacked and coplanar with the tpy ligand.

The minor isomer was isolated after purification on a neutral alumina column as a PF_6 salt. ESI-Mass revealed the molecular ion peak of [Ru(terpy)(L)Cl]$^+$ at m/z 552 and ^{1}H NMR immediately showed the existence of isomer (B) (Fig. 8). The 6py resonance is shifted upfield relative to isomer (A), as this H_6 atom is no longer deshielded by the choride atom. In addition,

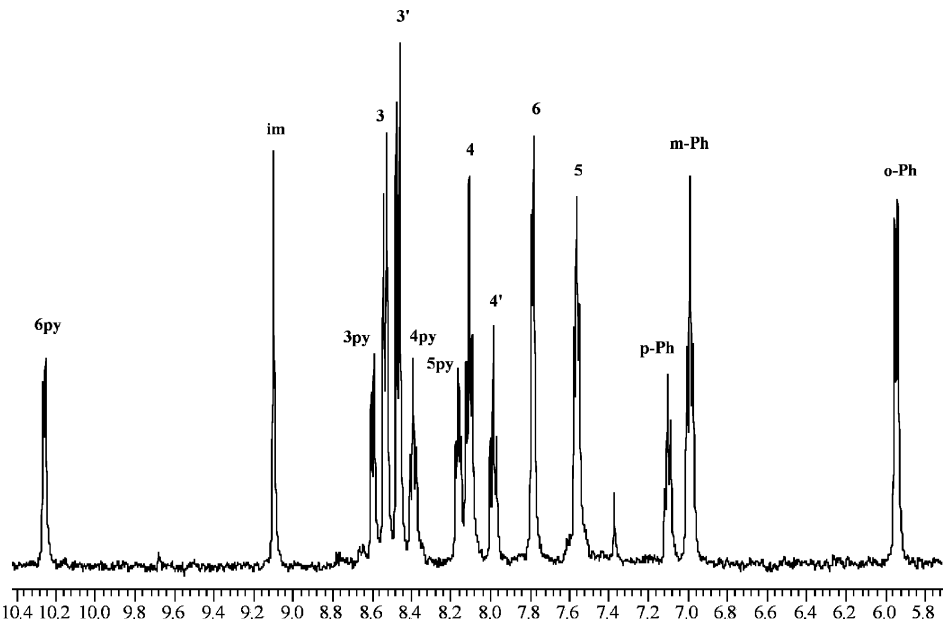

Fig. 7 500 MHz ^{1}H NMR of [Ru(tpy)(L)Cl][BF_4] in acetone-d_6 solution at 298 K.

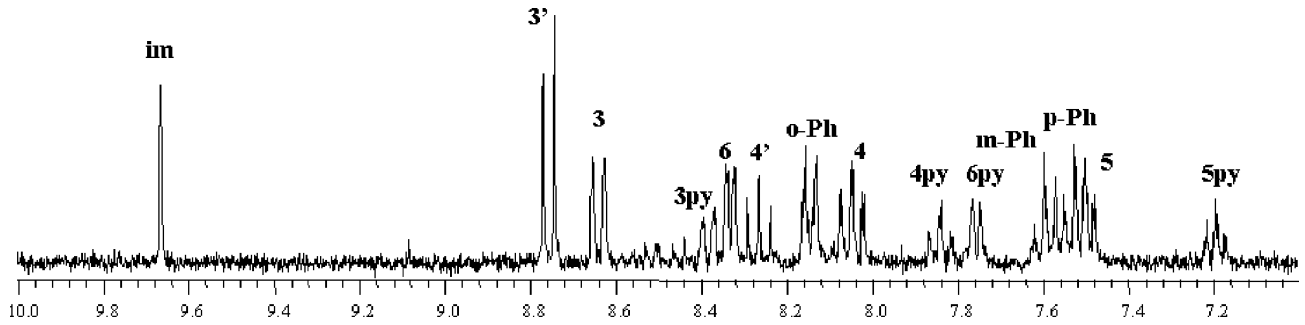

Fig. 8 300 MHz of minor isomer of [Ru(terpy)(L)Cl][PF_6] in acetone-d_6 at 298 K.

the *ortho* resonance shows a considerable downfield shift, as the *ortho* hydrogen atoms are now close to the chloride ligand. The full assignment has been achieved using integration values and 2D COSY NMR spectroscopy.

The isolation and characterisation of the minor isomer type (B) is unusual. From all complexes of the type {Ru(terpy)(L′)X}, with L′ = 2-phenylazopyridine, 2,2′-azobispyridine, pyridylimine or phenolic Schiff base, the main isomer type (A) (*i.e.* the isomer with the central pyridine ring of terpy *trans* to the pyridine ring of ligand L) is obtained.[14,20,24] Only in one case of a {Ru(terpy)(L′)X} complex with L′ = 2-phenylazopyridine has the minor isomer has been isolated, but was not fully characterised.[23] In the case of a methylated 2-phenylazopyridine compound[21] the existence of the minor isomer was also mentioned but attempts to isolate the minor isomer failed.

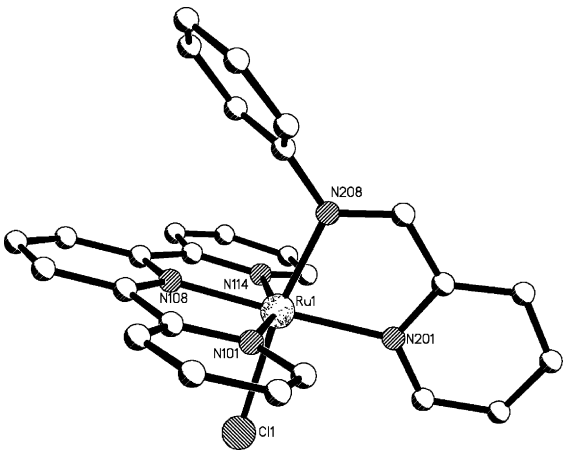

Fig. 9 Structure of the cations in the crystal structure of **2** (isomer A).

Recrystallisation of isomer (A) by slow diffusion of benzene into an acetone solution of the salt afforded crystals suitable for X-ray crystallography. The cation is of isomer type (A) and the ruthenium(II) centre occupies a distorted octahedral geometry, coordinating to one terdentate tpy ligand, one didentate L ligand and one chloride (Fig. 9). The tpy ligand is constrained to occupy three *mer* coordination sites. The imine of the pyridylimine unit is located *trans* to the chloro group, and the phenyl ring is located above the central ring of the tpy ligand. The ruthenium–nitrogen bond lengths to the central ring of the tpy ligand (1.959 Å) are shorter than those to the terminal rings (2.065 and 2.064 Å) and these bond lengths and the associated bond angles are comparable with those observed in other ruthenium(II) terpyridyl systems.[8,37,39] The phenyl ring is twisted with respect to the pyridylimine units (55°) and positioned above the central ring of the tpy ligand. As in complex **1** the geometric constraints at the imine nitrogen mean that it is not stacked coplanar with (or perpendicular to) that pyridyl ring. The terpyridyl unit is essentially planar (torsion angles between rings 0–5°) as is the pyridylimine units (torsion angle 3°). The bond from the ruthenium to the pyridine nitrogen of the pyridylimine ligand (2.073 Å) is similar to those in **1** and again that to the imine nitrogens is slightly shorter (2.020 Å). These distances are in correspondence with an analogous [Ru(terpy)(L′)Cl]ClO_4 complex (L′ = $NC_5H_4C(H)=N(C_6H_4)NH_2$).[15]

The cations are packed into chains through π–π and CH · · · π interactions as illustrated in Fig. 10. Each cation forms two types of intra-chain links. On one side of the cation a double ring

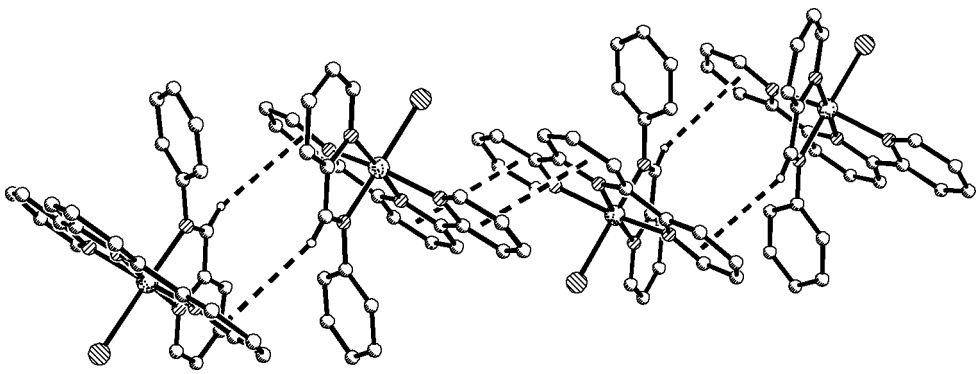

Fig. 10 Packing of the cations in the crystal structure of **2** (isomer A) through π–π and CH · · · π interactions. For clarity only the imine hydrogens are shown.

π-stack is formed between the tpy ligand and the corresponding ligand on the adjacent cation (centroid–centroid 3.78 Å). On the other side two CH · · · π interactions are formed involving the imine CH and the pyridine ring of the tpy which was not involved in the double ring π-stack (CH · · · centroid 3.12, 3.23 Å; C · · · centroid 3.96, 4.06 Å; ∠CH · · · centroid 149, 145°). The chains are packed together to form 2D sheets with disordered solvent and anions between these sheets. The anions make short contacts with cation protons and some additional (but less extensive) face–edge π contacts are observed between chains.

The electrochemical behaviour of the complex in acetonitrile solution has been examined by cyclic voltammetry. The complex exhibits a reversible oxidation process close to +0.50 V (*vs.* Fc/Fc^+) corresponding to the ruthenium(II)/(III) couple. As in complex **1** this value is slightly higher than the observed values in the corresponding bpy complexes[38] of 0.45 V for $[Ru(tpy)(Phbpy)Cl]^+$ and 0.42 V for $[Ru(tpy)(bpy)Cl]^+$, consistent with the ligand acting as a more effective π-acceptor. A reversible reduction is observed at −1.60 V, and two semi-reversible reductions at −1.85 and −2.15 V (*vs.* Fc/Fc^+). As in complex **1**, the first reduction (pyridylimine based) is again more facile than in the corresponding bpy complex.

The ^{1}MLCT absorption of **2** has a peak maximum at 520 nm (ε = 12 000 $dm^3\ mol^{-1}\ cm^{-1}$) which is around 15 nm red shifted in comparison with other mixed ligand Ru(II) terpyridyl complexes (λ = 502 nm (ε = 11 000 $dm^3\ mol^{-1}\ cm^{-1}$) for $[Ru(tpy)(bpy)Cl]^+$ and at λ = 508 nm (ε = 10 700 $dm^3\ mol^{-1}\ cm^{-1}$) for $[Ru(tpy)(Phbpy)Cl]^+$).[38] However, this may be due to a non-symmetrical spectral envelope which indicates the presence of two overlapping bands. The complex does not emit at room temperature, indicating that the pyridylimine ligand L does not alter the energy of the MC state responsible for deactivation of the ^{3}MLCT emission in Ru(II) terpyridyl complexes. The samples used for the emission studies were single-crystal samples and did not show emission at 77 K in ethanol–methanol (4 : 1) frozen glass. In one non-single-crystalline sample we did observe an emission at 77 K in ethanol–methanol (4 : 1) frozen glass with a maximum at 595 nm. Emission at this wavelength has been reported for a similar terpyridine–imine complex.[15] However, the 595 nm emission is strongest on irradiation at 475 nm (not 520 nm; the absorption maximum of complex **2**). Since $[Ru(tpy)(bpy)Cl]^+$ itself does emit at low *T* but at much longer wavelength (692 nm),[5] we propose that this 595 nm emission is not inherent emission from **2** but rather from a trace impurity of $[Ru(tpy)_2]^{2+}$ (λ_{em}= 596 nm; λ_{abs} = 470/475 nm)[5] in that particular non-single-crystalline sample.

Conclusion

We have demonstrated that *N*-aryl pyridylimine units can be used as structural alternatives to bipyridine units for constructing ruthenium(II) complexes. The crystal structures reveal that these *N*-arylpyridylimines are quite different from the 6-aryl-2,2′-bipyridines because the aryl group does not interfere with coordination of the imino nitrogen to the metal centre. They also do not introduce the cyclometallation possibilities associated with 6-aryl-2,2′-bipyridines and which complicates the chemistry of those ligands[38] (a disfavoured 4-membered chelate ring would be required for cyclometallation of an *N*-aryl pyridylimine). In this sense the *N*-aryl pyridylimines are structurally more like 2,2′-bipyridines than 6-aryl-2,2′-bipyridines. On coordination the *N*-aryl ring is positioned in such a way that it does not face–face π-stack with the other aryl rings in the complex; it is thus able to rotate freely in solution. The results confirm that units based on pyridylimine ligands may indeed be suitable for incorporation into nano-scale electronic or photonic arrays as we hoped. Both compounds **1** and **2** display reversible redox behaviour similar to the corresponding bipyridine analogues. **1** displays room temperature emission in the far-red region of the visible spectrum and shifted to longer wavelength than the corresponding bipyridine analogues. Pyridylimine units are thus attractive because of their ease of synthesis and because of their inherent emission profiles. We are currently exploring the incorporation of these units into polynuclear arrays.

Experimental

General

The complexes *cis*-$[Ru(bipy)_2Cl_2]\cdot 2H_2O$[40] and $[Ru(tpy)Cl_3]$[37] were prepared according to literature methods. Commercially available solvents and reagents were used without further purification. NMR spectra were recorded on Bruker DPX 300 and DRX 500 instruments using standard Bruker software. FAB mass spectra were recorded on a Micromass Autospec spectrometer using 3-nitrobenzyl alcohol as matrix. ESI-MS spectra were recorded on a Bruker Esquire 2000 in an acetonitrile solution. Microanalyses were conducted on a Leeman Labs CE44 CHN analyser by Warwick Analytical Service. Infrared spectra were recorded on a Perkin-Elmer Paragon 1000 instrument with the sample as solid pellets. UV-Vis spectra were recorded on a Perkin-Elmer Lambda 25 instrument. The luminescence studies were performed on a Photon Technology International QM-1 steady state spectrometer employed with a dual grating 500/750 nm emission monochromator and equipped with a 75 W xenon arc lamp and a model 810 photon counting detection system with a red-sensitive R928 photomultiplier tube. The data were collected and analysed with Felix software. Electrochemical measurements were performed using an EcoChemie μAutolab electrochemical workstation and standard GPES software. A conventional three-electrode configuration was used, with platinum working and auxiliary electrodes and a Ag/Ag^+ reference. The measurements were conducted in acetonitrile solution with 0.1 M $[n\text{-}Bu_4N][PF_6]$ base electrolyte. Potentials are quoted *vs.* ferrocene/ferrocenium couple (Fc/Fc^+ = 0.0 V) and all potentials were referenced to internal ferrocene added at the end of each experiment.

Phenyl-pyridin-2-ylmethylene-amine (L). Phenylamine (0.536 g, 5 mmol) and pyridine-2-carbaldehyde (0.466 g, 5 mmol) were stirred in benzene (15 ml) at room temperature for 3 h, in the presence of 3 Å molecular sieves. After cooling and removal of the molecular sieves, the solvent was evaporated *in vacuo*. The product is not pure and is a yellow oil. Yield 0.84 g (92%). FAB-MS: m/z = 183 $[MH]^+$. ^{1}H NMR 300 MHz (acetone-d_6): δ = 8.71 (d, 1 H, H_6), 8.58 (s, 1 H, H_{im}), 8.22 (d, 1 H, H_3), 7.94 (t, 1 H, H_4), 7.49 (t, 1 H, H_5), 7.45 (t, 2 H, *m*-Ph), 7.32 (d, 2 H, *o*-Ph), 7.29 (t, 1 H, *p*-Ph) ppm. ^{13}C NMR (acetone-d_6): δ = 207.1 (br), 162.7, 151.6, 138.5, 131.1, 128.5, 127.2, 122.9, 122.8

[Ru(bipy)$_2$L](PF$_6$)$_2$ (1). A mixture of *cis*-[Ru(bipy)$_2$Cl$_2$]·2H$_2$O (0.104 g, 0.2 mmol) and phenyl-pyridin-2-ylmethylene-amine (**L**) (0.055 g, 0.3 mmol) in methanol (65 ml) was heated at reflux under nitrogen for 4 h. After cooling at room temperature, the solution was filtered through celite and the filtrate was treated with an excess of methanolic NH_4PF_6 solution. The solvent was removed *in vacuo* to approximately 20 ml and the solution was cooled to 5 °C overnight. The brown-red product was collected on a porosity 4 sintered-glass filter and air dried. Recrystallisation from acetonitrile by slow diffusion of diisopropyl ether afforded crystals suitable for X-ray analysis. Yield 0.104 g (58%). $RuC_{32}H_{26}N_6P_2F_{12}\cdot 1H_2O$: calc. C 42.5, H 3.1, N 9.3; found C 42.4, H 2.8, N 9.2%. FAB-MS: m/z = 741 [M − PF$_6$]$^+$, 596 [M − 2PF$_6$]$^+$. UV-Vis (MeCN): 477 (ε = 9 000), 442 (ε = 9 000) and 285 nm (ε = 40 000 dm^3 mol^{-1} cm^{-1}). IR: 3082 m, 1603 s, 1572 w, 1545 m, 1488 m, 1466 s, 1446 s, 1426 w, 1314 m, 1297 w, 1274 w, 1242 m, 1200 w, 1160 m, 826 s, 757 s. ^{1}H NMR 500 MHz (acetone-d$_6$): δ = 9.43 (s, 1H, H$_{im}$), 8.94 (d, 1H, H$_{6a}$), 8.87 (d, 1H, H$_{3a}$), 8.86 (d, 1H, H$_{3b}$), 8.59 (d, 1H, H$_{3py}$), 8.55 (d, 1H, H$_{3c}$), 8.34 (d, 1H, H$_{3d}$), 8.31 (t, 1H, H$_{4a}$), 8.25 (m, 3H, H$_{4c}$, H$_{4py}$, H$_{4b}$), 8.17 (d, 1H, H$_{6py}$), 8.09 (d, 1H, H$_{6b}$), 8.04 (d, 1H, H$_{6c}$), 7.94 (m, 2H, H$_{6d}$, H$_{4d}$), 7.76 (t, 1H, H$_{5a}$), 7.71 (t, 1H, H$_{5c}$), 7.67 (t, 1H, H$_{5py}$), 7.57 (t, 1H, H$_{5b}$), 7.40 (t, 1H, H$_{5d}$), 7.20 (t, 1H, *o*-Ph), 7.10 (t, 2H, *m*-Ph), 6.79 (d, 2H, *o*-Ph).

[Ru(tpy)LCl]BF$_4$ (2, isomer A). [Ru(tpy)Cl$_3$] (0.044 g, 0.1 mmol) and phenyl-pyridin-2-ylmethylene-amine (L) (0.018 g, 0.1 mmol) were added in methanol (25 ml) containing a few drops of 4-ethylmorpholine. The mixture was heated at reflux for 4 h. After cooling to room temperature the solution was concentrated by rotary evaporation to approximately 15 ml. The solution was then treated with an excess of methanolic NH_4BF_4 solution. The resultant dark purple precipitate was collected on a porosity 4 sintered-glass filter and dried in the air. Recrystallisation from acetone by slow diffusion of benzene afforded crystals suitable for X-ray analysis. Yield 0.022 g (34%). $RuC_{27}H_{21}N_5ClBF_4\cdot 2CH_3OH$: calc. C 49.5, H 3.8, N 9.7; found C, 49.6; H, 4.2; N, 10.0%; FAB-MS: m/z = 552 [M − BF$_4$]$^+$. UV-Vis (MeCN): 274 (ε = 23 000), 314 (ε = 31 000) and 523 nm (ε = 12 000 dm^3 mol^{-1} cm^{-1})

IR: 3064 m, 3032 m, 1634 w, 1599 m, 1563 w, 1525 m, 1466 m, 1447 s, 1434 s, 1385 s, 1282 m, 1247 m, 1201 w, 1160 w, 1049 s, 1032 s, 763 s, 697 s. ^{1}H NMR (acetone-d$_6$): δ = 10.26 (d, 1H, H$_{6py}$), 9.10 (s, 1H, H$_{im}$), 8.59 (d, 1H, H$_{3py}$), 8.53 (d, 2H, H$_{3tpy}$), 8.47 (d, 2H, H$_{3'tpy}$), 8.39 (t, 1H, H$_{4py}$), 8.16 (t, 1H, H$_{5py}$), 8.11 (t, 2H, H$_{4tpy}$), 7.98 (t, 1H, H$_{4'tpy}$), 7.79 (d, 2H, H$_{6tpy}$), 7.56 (d, 2H, H$_{5tpy}$), 7.10 (t, 1H, *o*-Ph), 6.99 (t, 2H, *m*-Ph), 5.94 (d, 2H, *o*-Ph).

[Ru(tpy)LCl]PF$_6$ (2, isomer B). This was synthesized in an analogous fashion, but use of NH_4PF_6 instead of NH_4BF_4 and used for separation of the two isomers.

The solid, dissolved in acetone was put on a neutral alumina column and acetone was used as an eluent. Fractions of *ca.* 10 ml were collected. The first two fractions contained pure isomer (A), whereas fractions 5 and 6 contained pure isomer (B). ESI-Mass: m/z = 552 [M − PF$_6$]$^+$.

^{1}H NMR 300 MHz (acetone-d$_6$): δ = 9.67 (s, 1H, H$_{im}$), 8.76 (d, 2H, H$_{3'tpy}$), 8.638 (d, 2H, H$_{3tpy}$), 8.40 (d, 1H, H$_{3py}$), 8.34 (d, 2H, H$_{6tpy}$), 8.27 (t, 1H, H$_{4'tpy}$), 8.13 (d, 2H, *o*-Ph), 8.05 (t, 2H, H$_{4tpy}$), 7.84 (t, 1H, H$_{4py}$), 7.77 (d, 1H, H$_{6py}$), 7.53 (m, 5H, *m*-Ph, *o*-Ph, H$_{5tpy}$).

X-Ray crystal structure determination of 1 and 2

X-Ray data for **1** and **2** were collected with a Siemens SMART three-circle system with a CCD area detector, with crystals held at 180 K with the Oxford Cryostream Cooler.[41]

There were no systematic absences. Space groups (both $P\bar{1}$) were chosen on the basis of intensity statistics and shown to be correct by successful refinement. The structures were solved by direct methods[42] with additional light atoms found by Fourier methods. Hydrogen atoms were added at calculated positions and refined using a riding model. Anisotropic displacement parameters were used for all non-H atoms; H atoms were given isotropic displacement parameters equal to 1.2 times the equivalent isotropic displacement parameter of the atom to which the H atom was attached. Pertinent data for each of the structure determinations are given in Table 2, and bond lengths and angles in Tables 3 and 4.

1. The asymmetric unit contains one complete complex and two PF$_6$ counterions.

2 (isomer A). The asymmetric unit contains one complex comprised of an Ru bound to a terpy and a pyridine imine ligand. There is a molecule of benzene which is disordered over two positions (55 : 45 occupancy). Both parts were refined anisotropically but still have large thermal parameters. The BF$_4$ counter ions also disordered around the B10–F11 axis with both positions refined anisotropically (min : major 2 : 8).

CCDC reference numbers 293457 and 293458.

For crystallographic data in CIF or other electronic format see DOI: 10.1039/b518027a

Table 2 Crystallographic data for crystal structure determinations of **1** and **2** (isomer A)

Compound	**1**	**2** (isomer A)
Formula	$C_{32}H_{26}N_6RuP_2F_{12}$	$C_{33}H_{27}N_5ClRuBF_4$
Formula weight/g mol^{-1}	885.60	716.93
Crystal system	Triclinic	Triclinic
Space group	$P\bar{1}$	$P\bar{1}$
a/Å	9.0813(8)	11.0703(12)
b/Å	10.6974(9)	11.8803(13)
c/Å	17.7534(14)	13.2873(15)
α/°	87.438(2)	92.061(8)
β°	85.6830(10)	110.294(10)
γ°	83.579(2)	104.768(11)
V/Å^3	1707.9(2)	1569.9(3)
D_c/g cm^{-3}	1.722	1.517
Z	2	2
μ[Mo Kα]/mm^{-1}	0.653	0.640
Crystal color	Orange	Purple
Crystal size/mm	0.2 × 0.12 × 0.01	0.38 × 0.20 × 0.16
Total data	10813	10104
Total unique data	7717	7236
R_{int}	0.0739	0.0300
No. of refined parameters	478	432
$R1^a$ [$I > 2\sigma(I)$]	0.0854 [3414 refl.]	0.0271 [7824 refl.]
w$R2^b$ (all data)	0.1716	0.0631
GoF	0.964	1.020

^{a} $R1 = \sum||F_o| - |F_c||/\sum|F_o|$. ^{b} $wR2 = [\sum[w(F_o^2 - F_c^2)^2]/\sum[w(F_o^2)^2]]^{1/2}$.

Table 3 Selected bond distances (Å) and angles (°) of **1**

Ru(1)–N(308)	2.045(6)	N(301)–Ru(1)–N(101)	95.2(3)
Ru(1)–N(301)	2.056(6)	N(201)–Ru(1)–N(101)	95.4(3)
Ru(1)–N(201)	2.057(6)	N(308)–Ru(1)–N(112)	98.9(2)
Ru(1)–N(101)	2.061(7)	N(301)–Ru(1)–N(112)	173.4(3)
Ru(1)–N(112)	2.070(6)	N(201)–Ru(1)–N(112)	84.6(2)
Ru(1)–N(212)	2.077(6)	N(101)–Ru(1)–N(112)	78.4(3)
		N(308)–Ru(1)–N(212)	98.8(3)
N(308)–Ru(1)–N(301)	78.6(2)	N(301)–Ru(1)–N(212)	90.2(2)
N(308)–Ru(1)–N(201)	176.0(3)	N(201)–Ru(1)–N(212)	79.0(3)
N(301)–Ru(1)–N(201)	98.0(2)	N(101)–Ru(1)–N(212)	172.8(3)
N(308)–Ru(1)–N(101)	87.0(2)	N(112)–Ru(1)–N(212)	96.3(3)

Table 4 Selected bond distances (Å) and angles (°) of **2** (isomer A)

Ru(1)–N(108)	1.959(4)	N(114)–Ru(1)–N(101)	158.59(16)
Ru(1)–N(208)	2.020(4)	N(108)–Ru(1)–N(201)	176.50(15)
Ru(1)–N(114)	2.064(4)	N(208)–Ru(1)–N(201)	77.46(15)
Ru(1)–N(101)	2.065(4)	N(114)–Ru(1)–N(201)	100.31(17)
Ru(1)–N(201)	2.073(4)	N(101)–Ru(1)–N(201)	101.10(16)
Ru(1)–Cl(1)	2.4052(12)	N(108)–Ru(1)–Cl(1)	89.86(11)
		N(208)–Ru(1)–Cl(1)	170.07(12)
N(108)–Ru(1)–N(208)	99.07(15)	N(114)–Ru(1)–Cl(1)	87.50(11)
N(108)–Ru(1)–N(114)	79.61(16)	N(101)–Ru(1)–Cl(1)	91.36(11)
N(208)–Ru(1)–N(114)	98.32(15)	N(201)–Ru(1)–Cl(1)	93.63(11)
N(108)–Ru(1)–N(101)	86.13(15)		

Acknowledgements

This work was supported by an EU Marie Curie Training Site Fellowship (N.M.; HPMT-GH-01-00365-02), Marie Curie EU Research Training Networks (UNI-NANOCUPS MRTN-CT-2003-504233; MARCY HPRN-CT-2002-00175) and the EPSRC (J.F.). We thank EPSRC and Siemens Analytical Instruments for grants in support of the diffractometer, the Royal Society for provision of an electrochemical workstation (M.J.H.), the EPSRC National Mass Spectrometry Service Centre, Swansea for recording the electrospray mass spectra and Drs A. J. Clarke and N. Spencer for assistance with NMR studies. We thank the referees for their helpful suggestions. This work was conducted in the context of COST D31 (WG D31/001/04). M.J.H. is the Royal Society of Chemistry Sir Edward Frankland Fellow 2004–5.

References

1 G. Van Koten and K. Vrieze, *Adv. Organomet. Chem.*, 1982, **21**, 151.
2 E. C. Constable, *Adv. Inorg. Chem.*, 1989, **34**, 1.
3 L. J. Childs, N. W. Alcock and M. J. Hannon, *Angew. Chem., Int. Ed.*, 2002, **41**, 4244; F. Tuna, J. Hamblin, G. Clarkson, W. Errington, N. W. Alcock and M. J. Hannon, *Chem.–Eur. J.*, 2002, **8**, 4957; J. Hamblin, A. Jackson, N. W. Alcock and M. J. Hannon, *J. Chem. Soc., Dalton Trans.*, 2002, 1635; L. J. Childs, N. W. Alcock and M. J. Hannon, *Angew. Chem., Int. Ed.*, 2001, **40**, 1079; M. J. Hannon, C. L. Painting and N. W. Alcock, *Chem. Commun.*, 1999, 2023; M. J. Hannon, S. Bunce, A. J. Clarke and N. W. Alcock, *Angew. Chem., Int. Ed.*, 1999, **38**, 1277; M. J. Hannon, C. L. Painting, A. Jackson, J. Hamblin and W. Errington, *Chem. Commun.*, 1997, 1807; F. Tuna, J. Hamblin, A. Jackson, G. Clarkson, N. W. Alcock and M. J. Hannon, *Dalton Trans.*, 2003, 2141; F. Tuna, G. Clarkson, N. W. Alcock and M. J. Hannon, *Dalton Trans.*, 2003, 2149.
4 E. Moldrheim, M. J. Hannon, I. Meistermann, A. Rodger and E. Sletten, *J. Biol. Inorg. Chem.*, 2002, **7**, 770; I. Meistermann, V. Moreno, M. J. Prieto, E. Moldrheim, E. Sletten, S. Khalid, P. M. Rodger, J. C. Peberdy, C. J. Isaac, A. Rodger and M. J. Hannon, *Proc. Natl. Acad. Sci. U. S. A.*, 2002, **99**, 5069; M. J. Hannon, V. Moreno, M. J. Prieto, E. Moldrheim, E. Sletten, I. Meistermann, C. J. Isaac, K. J. Sanders and A. Rodger, *Angew. Chem., Int. Ed.*, 2001, **40**, 880.
5 A. Juris, V. Balzani, F. Barigelletti, S. Campagna, P. Belser and A. von Zelewsky, *Coord. Chem. Rev.*, 1988, **84**, 85.
6 V. Balzani and F. Scandola, *Supramolecular Photochemistry*, Ellis Horwood, Chichester, 1991.
7 V. Balzani, S. Campagna, G. Denti, A. Juris, S. Serroni and M. Venturi, *Acc. Chem. Res.*, 1998, **31**, 26; V. Balzani, A. Juris, M. Venturi, S. Campagna and S. Serroni, *Chem. Rev.*, 1996, **96**, 759; L. DeCola, *Chimia*, 1996, **50**, 214; E. C. Constable, *Chem. Commun.*, 1997, 1073; S. Bernard, C. Blum, A. Beyeler, L. DeCola and V. Balzani, *Coord. Chem. Rev.*, 1999, **192**, 155; A. von Zelewsky and P. Belser, *Chimia*, 1998, **52**, 620; J.-P. Sauvage, J.-P. Collin, J.-C. Chambron, S. Guillerez and C. Coudret, *Chem. Rev.*, 1994, **94**, 993; M. Hissler, A. El-ghayoury, A. Harriman and R. Ziessel, *Angew. Chem., Int. Ed.*, 1998, **37**, 1717; M. D. Ward, *Chem. Soc. Rev.*, 1995, **24**, 121.
8 N. W. Alcock, P. R. Barker, J. M. Haider, M. J. Hannon, C. L. Painting, Z. Pikramenou, E. A. Plummer, K. Rissanen and P. Saarenketo, *J. Chem. Soc., Dalton Trans.*, 2000, 4702.
9 M. Silva, J. M. Haider, R. Heck, M. Chavarot, A. Marsura and Z. Pikramenou, *Supramol. Chem.*, 2003, **15**, 563; J. M. Haider, R. M. Williams, L. De Cola and Z. Pikramenou, *Angew. Chem., Int. Ed.*, 2003, **42**, 1830; J. M. Haider, M. Chavarot, S. Weidner, I. Sadler, R. M. Williams, L. De Cola and Z. Pikramenou, *Inorg. Chem.*, 2001, **40**, 3912; J. M. Haider and Z. Pikramenou, *Eur. J. Inorg. Chem.*, 2001, 189; S. Weidner and Z. Pikramenou, *Chem. Commun.*, 1998, 1473; H. Krass, E. A. Plummer, J. M. Haider, P. R. Barker, N. W. Alcock, Z. Pikramenou, M. J. Hannon and D. G. Kurth, *Angew. Chem., Int. Ed.*, 2001, **40**, 3862; J. M. Haider and Z. Pikramenou, *Chem. Soc. Rev.*, 2005, **34**, 120.
10 M. Zukalova, A. Zukal, L. Kavan, M. K. Nazeeruddin, P. Liska and M. Gratzel, *Nano Lett.*, 2005, **5**, 1789.
11 O. Bossart, L. De Cola, S. Welter and G. Calzaferri, *Chem.–Eur. J.*, 2004, **10**, 5771.
12 K. K. Patel, E. A. Plummer, M. Darwish, A. Rodger and M. J. Hannon, *J. Inorg. Biochem.*, 2002, **91**, 220; B. Onfelt, P. Lincoln and B. Norden, *J. Am. Chem. Soc.*, 2001, **123**, 3630; B. T. Farrer and H. H. Thorp, *Inorg. Chem.*, 2000, **39**, 44; J. G. Collins, A. D. Sleeman, J. R. Aldrich-Wright, I. Greguric and T. W. Hambley, *Inorg. Chem.*, 1998, **37**, 3133; P. Lincoln, E. Tuite and B. Norden, *J. Am. Chem. Soc.*, 1997, **119**, 1454; S. D. Choi, M. S. Kim, S. K. Kim, P. Lincoln, E. Tuite and B. Norden, *Biochemistry*, 1997, **36**, 214; J. K. Barton, *Pure Appl. Chem.*, 1989, **61**, 563; S. Satyanarayana, J. C. Dabrowiak and J. B. Chaires, *Biochemistry*, 1993, **32**, 2573.
13 M. Maruyama and Y. Kaizu, *Inorg. Chim. Acta*, 1996, **247**, 155.
14 B. Mondal, S. Chakraborty, P. Munshi, M. G. Walawalkar and G. K. Lahiri, *J. Chem. Soc., Dalton Trans.*, 2000, 2327.
15 N. Chanda, B. Mondal, V. G. Puranik and G. K. Lahiri, *Polyhedron*, 2002, **21**, 2033.
16 B. Mondal, V. G. Puranik and G. K. Lahiri, *Inorg. Chem.*, 2002, **41**, 5831.
17 S. Choudhury, A. K. Deb and S. Goswami, *J. Chem. Soc., Dalton Trans.*, 1994, 1305.
18 E. C. Constable, M. J. Hannon, A. M. W. Cargill Thomson, D. A. Tocher and J. V. Walker, *Supramol. Chem.*, 1993, **2**, 243; F. Y. Wu, E. Riesgo, A. Pavalova, R. A. Kipp, R. H. Schmehl and R. P. Thummel, *Inorg. Chem.*, 1999, **38**, 5620.
19 R. C. Chotalia, E. C. Constable, M. J. Hannon and D. A. Tocher, *J. Chem. Soc., Dalton Trans.*, 1995, 3571.
20 N. C. Pramanik, K. Pramanik, P. Ghosh and S. Bhattacharya, *Polyhedron*, 1998, **17**, 1525; K. Hansongnern, U. Saeteaw, J. Cheng, F. L. Liao and T. H. Lu, *Acta Crystallogr., Sect. C: Cryts. Struct. Commun.*, 2001, **C57**, 895; B. Mondal, H. Paul, V. G. Puranik and G. K. Lahiri, *J. Chem. Soc., Dalton Trans.*, 2001, 481.
21 B. Mondal, M. G. Walawalkar and G. K. Lahiri, *J. Chem. Soc., Dalton Trans.*, 2000, 4209.
22 K. Hansongnern, U. Saeteaw, G. Mostafa, Y. C. Jiang and T. H. Lu, *Anal. Sci.*, 2001, **17**, 683.
23 K. Hansongnern, U. Saeteaw and G. Mostafa, *Anal. Sci.*, 2003, **19**, 971.
24 E. Corral, A. C. G. Hotze, D. M. Tooke, A. L. Spek and J. Reedijk, *Inorg. Chim. Acta*, 2006, **359**, 830.
25 G. M. Brown, T. R. Weaver, F. R. Keene and T. J. Meyer, *Inorg. Chem.*, 1976, **15**, 190.
26 P. Belser and A. von Zelewsky, *Helv. Chim. Acta*, 1980, **63**, 1675.
27 E. V. Dose and L. J. Wilson, *Inorg. Chem.*, 1978, **17**, 2660.
28 V. W. W. Yam and V. W. M. Lee, *J. Chem. Soc., Dalton Trans.*, 1997, 3005.

29 E. S. Krider, J. J. Rack, N. L. Frank and T. J. Meade, *Inorg. Chem.*, 2001, **40**, 4002.
30 H. Brunner, J. Spitzer and B. Nuber, *Enantiomer*, 1999, **4**, 91.
31 D. P. Rillema, D. S. Jones and H. A. Levy, *J. Chem. Soc., Chem. Commun.*, 1979, 849.
32 A. C. G. Hotze, E. P. L. van der Geer, H. Kooijman, A. L. Spek, J. G. Haasnoot and J. Reedijk, *Eur. J. Inorg. Chem.*, 2005, 2648.
33 M. Maruyama and Y. Kaizu, *J. Phys. Chem.*, 1995, **99**, 6152.
34 The addition of DCl and NEt_4Cl to the complex in acetonitrile was also studied by NMR: addition of DCl caused the imine proton signal to shift slightly downfield from 9.02 ppm to 9.1 ppm. In addition, the signals assigned to the H_3 atoms of both bpy and pyridylimine ligands shift downfield (showing a shift at about 0.05 ppm). The shift of the signals might be caused by the change in intermolecular hydrogen bonding. No new signals appear in the NMR indicating that the compound remains stable, or that any new compounds are present at low concentration. To confirm that exchange effects are not masking new species the sample was cooled down. At −50 °C no new signals could be distinguished. These NMR results indicate that under these conditions (but without irradiation) the sample remains stable. Addition of some NEt_4Cl to the sample also resulted in a slight shifting of the signals and without the appearance of any new signals. The shifts are slightly more pronounced than in the case of addition of DCl.
35 See for example: H. P. Hughes, D. Martin, S. Bell, J. J. McGarvey and J. G. Vos, *Inorg. Chem.*, 1993, **32**, 4402; R. Arakawa, L. Jian, A. Yoshimura, K. Nozaki, T. Ohno, H. Doe and T. Matsuo, *Inorg. Chem.*, 1995, **34**, 3874; E. Baranoff, J.-P. Collin, J. Furusho, Y. Furusho, A.-C. Laemmel and J.-P. Sauvage, *Inorg. Chem.*, 2002, **41**, 1215; E. Baranoff, J.-P. Collin, Y. Furusho, A.-C. Laemmel and J.-P. Sauvage, *Chem. Commun.*, 2000, 1935; P. J. Steel, F. Lahousse, D. Lerner and C. Marzin, *Inorg. Chem.*, 1983, **22**, 1488; B. Durham, J. L. Walsh, C. L. Carter and T. J. Meyer, *Inorg. Chem.*, 1980, **19**, 860.
36 S. Tachiyashiki, H. Ikezawa and K. Mizumachi, *Inorg. Chem.*, 1994, **33**, 623. This paper reports a monodentate intermediate formed on photoirradiation of a tris-diimine complex containing 3,3′dimethyl-2,2′bipyridine and notes that acid stabilises the monodentate intermediate.
37 E. C. Constable, A. M. W. Cargill Thomson, M. A. M. Daniels and D. A. Tocher, *New J. Chem.*, 1992, **16**, 855.
38 E. C. Constable and M. J. Hannon, *Inorg. Chim. Acta*, 1993, **211**, 1011.
39 E. C. Constable, C. E. Housecroft, M. Neuberger, A. G. Schneider and M. Zehnder, *J. Chem. Soc., Dalton Trans.*, 1997, 2427; K. Lashgari, M. Kritikos, R. Norrestam and T. Norrby, *Acta Crystallogr., Sect. C: Cryts. Struct. Commun.*, 1999, **C55**, 64; M. Beley, J.-P. Collin, R. Louis, B. Metz and J.-P. Sauvage, *J. Am. Chem. Soc.*, 1991, **113**, 8521; K. L. Bushell, S. M. Couchman, J. C. Jefferey, L. H. Rees and M. D. Ward, *J. Chem. Soc., Dalton Trans.*, 1998, 1998; M. Ziegler, M. Monney, H. Stoeckli-Evans, A. von Zelewsky, I. Sasaki, G. Dupic, J.-C. Daran and G. A. Balavoine, *J. Chem. Soc., Dalton Trans.*, 1999, 667.
40 B. P. Sullivan, D. J. Salmon and T. J. Meyer, *Inorg. Chem.*, 1978, **17**, 3334.
41 J. Cosier and A. M. Glazer, *J. Appl. Crystallogr.*, 1986, **19**, 105.
42 G. M. Sheldrick, *Acta Crystallogr., Sect. D: Biol. Crytallogr.*, 1990, **D49**, 18.

